

Nonstationary heat conduction in one-dimensional models with substrate potentialO. V. Gendelman,^{1,*} R. Shvartsman,¹ B. Madar,¹ and A. V. Savin²¹*Faculty of Mechanical Engineering, Technion–Israel Institute of Technology, Haifa 32000, Israel*²*Semenov Institute of Chemical Physics, Russian Academy of Sciences, RU-117977 Moscow, Russia*

(Received 14 August 2011; published 3 January 2012)

The paper investigates nonstationary heat conduction in one-dimensional models with substrate potential. To establish universal characteristic properties of the process, we explore three different models: Frenkel-Kontorova (FK), ϕ^4+ (ϕ^4+), and ϕ^4- (ϕ^4-). Direct numeric simulations reveal in all these models a crossover from oscillatory decay of short-wave perturbations of the temperature field to smooth diffusive decay of the long-wave perturbations. Such behavior is inconsistent with the parabolic Fourier equation of heat conduction and clearly demonstrates the necessity for hyperbolic corrections in the phenomenological description of the heat conduction process. The crossover wavelength decreases with an increase in the average temperature. The decay patterns of the temperature field almost do not depend on the amplitude of the perturbations, so the use of linear evolution equations for the temperature field is justified. In all models investigated, the relaxation of thermal perturbations is exponential, contrary to a linear chain, where it follows a power law. The most popular lowest-order hyperbolic generalization of the Fourier law, known as the Cattaneo-Vernotte or telegraph equation, is also not valid for the description of the observed behavior of the models with the substrate potential, since the characteristic relaxation time in an oscillatory regime strongly depends on the excitation wavelength. For some of the models, this dependence seems to obey a simple scaling law.

DOI: [10.1103/PhysRevE.85.011105](https://doi.org/10.1103/PhysRevE.85.011105)

PACS number(s): 05.60.-k, 44.10.+i, 05.45.-a, 05.70.Ln

I. INTRODUCTION

The relationship between empiric equations of heat conduction (Fourier law) and the microstructure of solid dielectrics is known to be one of the oldest and most elusive unsolved problems in solid state physics [1,2]. The classic solution for the problem suggested by Peierls [3] was questioned after the seminal numeric experiment of Fermi, Pasta, and Ulam [4], which disproved the common belief concerning fast thermalization and mixing in nonintegrable systems with weak nonlinearity. Despite the large amount of work done, the necessary and sufficient conditions for a microscopic model of a solid to obey macroscopically the Fourier law with finite and size-independent heat conduction coefficients [4–16] are not known yet. Numerous anomalies in the heat transfer in microscopic models of dielectrics were revealed by means of direct numeric simulation over recent years, including the qualitatively different behavior of models of different types (with and without the substrate potential) and dimensionality [1]. To date, it is believed that in one dimension in microscopic models with conserved momentum, the heat conduction coefficient diverges in the thermodynamic limit (as the chain length N goes to infinity) as $\kappa \sim N^\gamma$ with γ varying in the interval 0.3–0.4 [1]. The only known exception with a convergent heat conduction coefficient is a chain of coupled rotators [8,9]. As for the models without the moment conservation, their heat conduction is convergent [10,14], with the exception of integrable models [11]. In two dimensions, the divergence still exists [1], although it is reported to be of logarithmic rather than power-law type. It is believed that in three dimensions the heat conduction coefficient will converge, although some alternative data exist [15,16].

The vast majority of results obtained to date in the field of microscopic foundations of heat conduction dealt with stationary problem, with steady heat flux under constant thermal gradient. In all these cases the macroscopic law to be verified was the common Fourier law of heat conduction. However, it is well known that due to its parabolic character it implies infinite speed of the signal propagation and thus should be modified if very large gradients or extremely small scales are involved [17–20]. On a macroscopic level, numerous modifications were suggested to recover the hyperbolic character of the heat transport equation [19–22]. Perhaps, the most known is the lowest-order approximation known as the Cattaneo-Vernotte (CV) or telegraph (TE) law [23,24]. It is written as

$$\left(1 + \tau \frac{\partial}{\partial t}\right) \vec{q} = -\kappa \vec{\nabla} T, \quad (1)$$

where κ is the standard heat conduction coefficient, τ is the characteristic relaxation time of the system, \vec{q} is the vector of heat flux, and T is the temperature. The relaxation time is rather short for majority of materials (10^{-12} s at room temperature), but can be of order 1 s, for instance, in some biological tissues [25].

Modifications of the Fourier law bring about new observable physical phenomena, such as temperature waves or the second sound [17–20]. The importance of hyperbolic heat conduction models for the description of nanoscale heat transfer has been recognized in recent experiments [26,27].

Only a few papers have dealt with microscopic foundations of non-Fourier heat conduction laws from the first principles or by its numeric investigation in the microscopic models [26,28–37]. These works confirm that the non-Fourier effects may be very significant if large space gradients or fast changes of the temperature are involved.

In a recent paper [38] an attempt was made to relate the structure and parameters of microscopic models with

*ovgend@tx.technion.ac.il

conserved momentum to empiric description of the non-Fourier heat conduction. For this sake, two models belonging to different universality classes with respect to the stationary heat conduction were studied: the β -Fermi-Pasta-Ulam (FPU) chain and the chain of rotators. Oscillatory behavior of the decaying temperature disturbance, compatible only with a hyperbolic macroscopic equation of thermal transport, has been revealed in both models. The CV equation of the heat transport adequately describes the behavior of the chain of rotators, besides the region of crossover between the hyperbolic and the parabolic behavior. However, the β -FPU model does not obey the CV equation.

This paper continues the line of research started in Ref. [38] and investigates the relationship between structure, parameters, and macroscopic description of the nonstationary heat transfer in models with the substrate (on-site) potential. Such models are known to have normal heat conductivity [1,9,10,14]. We are going to check (a) whether the effects of hyperbolicity can be observed in such models, (b) whether the thermal transport in these models can be described by linear equations, and (c) to what extent the behavior of these model with on-site potential is universal and what one can say about suitable macroscopic phenomenological models.

II. MODELS AND PROCEDURES

Stationary heat transfer is characterized by a single coefficient of heat (or thermal) conductivity. In numeric experiments it is measured either by direct simulation of the stationary flux under constant temperature gradient, or from autocorrelation of the heat flux in an isolated system via the Green-Kubo formula [1]. The nonstationary conduction involves at least two parameters (CV equation) or even more in more advanced models. Moreover, one should not be bound by *a priori* selection of the empiric equation to fit the results. Then, it is desirable to find the characteristics of the process which can be measured directly from the numeric data and are not related to specific choice of the macroscopic empiric equation.

One such choice may be observation of the temperature waves (the second sound), implemented, for instance, in papers [27,35–37]. We follow here a different approach [38] based on the study of relaxation patterns for different spatial modes of the temperature field. Simply put, if one initiates the sinusoidal temperature profile in the system and then removes all external forces, the system will relax to uniform temperature distribution; temporal profile of this relaxation is of main interest. In particular, the oscillatory relaxation pattern is naturally related to the hyperbolicity of the system and is qualitatively inconsistent with the Fourier law [38]. Such an approach is related to early numeric simulations of the nonstationary heat conduction in argon crystals [30] and of thermal conductivity in superlattices [34].

Moreover, careful analysis of the relaxation profiles for different modes of temperature perturbation also can provide interesting insights. For instance, Eq. (1) leads to the prediction that all spatial temperature modes which have oscillatory decay will have the same characteristic relaxation time [38]. One can verify this prediction by comparison with the numeric data and thus to evaluate the accuracy of the CV equation (or any other model equation) for a particular model.

For a general one-dimensional model with on-site potential, we simulate the chain of particles with unit masses with the Hamiltonian

$$H = \sum_{n=1}^N [p_n^2/2 + V(u_{n+1} - u_n) + U(u_n)]. \quad (2)$$

Here u_n is the displacement of the n th particle, $p_n = \dot{u}_n$, $V(\rho)$ is the potential of the nearest-neighbor interaction, and $U(u)$ is the on-site potential [the minimum of $V(\rho)$ corresponds to $\rho = 0$, and the minimum of $U(u)$ is at $u = 0$]. The global minimum of the potential energy corresponds to an unperturbed state $\{u_n = 0\}_{n=1}^N$. Boundary conditions are adopted to be periodic.

In order to obtain the initial nonequilibrium temperature distribution, each particle in the chain has been initially connected to a separate Langevin thermostat. For this sake, the following system of equations was simulated:

$$\begin{aligned} \ddot{u}_n &= V'(u_{n+1} - u_n) - V'(u_n - u_{n-1}) - U'(u_n) \\ &\quad - \gamma \dot{u}_n + \xi_n, \quad n = 1 \dots N, \end{aligned} \quad (3)$$

where γ is the damping coefficient and the white noise ξ_n is normalized by the following conditions:

$$\langle \xi_n(t) \rangle = 0, \quad \langle \xi_n(t_1) \xi_m(t_2) \rangle = 2\gamma T_n \delta_{nm} \delta(t_1 - t_2), \quad (4)$$

where T_n is the prescribed temperature of the n th particle.

In order to study the relaxation of different spatial modes of the initial temperature distribution, its profile has been prescribed as

$$T_n = T_0 - A \cos[2\pi(n-1)/Z], \quad (5)$$

where T_0 is the average temperature, A is the amplitude of the perturbation, and Z is the length of the mode (number of particles). The overall length of the chain N has to be a multiple of Z in order to satisfy the periodic boundary conditions. After the initial heating in accordance with Eqs. (3)–(5), the Langevin thermostats were removed and relaxation of the isolated system to a stationary temperature profile was studied. The results were averaged over about 10^6 – 10^7 realizations of the initial profile $\{T_n\}_{n=1}^N$ in order to reduce the effect of fluctuations.

In this paper, we analyze three models with linear nearest-neighbor interactions, which differ by the shape of the on-site potential. The Hamiltonians of all three models are written as

$$H = \sum_{n=1}^N [p_n^2/2 + (u_{n+1} - u_n)^2/2 + U(u_n)]. \quad (6)$$

The unit coefficient of the parabolic potential of the nearest-neighbor interaction does not effect the generality. We treat three different on-site potentials: sinusoidal potential (Frenkel-Kontorova model, FK)

$$U(u) = 1 - \cos u; \quad (7)$$

ϕ^4 – potential

$$U(u) = 2u^2(u - 2\pi)^2/\pi^4; \quad (8)$$

ϕ^4 + potential

$$U(u) = u^2/2 + u^4/4. \quad (9)$$

Substrate potentials (7)–(9) differ topologically. The FK potential is periodic and bounded. Potential ϕ^4_- is double-well and unbounded. To simplify the comparison, a distance between the well minima and a height of the potential barrier are the same as for the FK model. Potential ϕ^4_+ is single-well and unbounded.

III. RESULTS

The first set of simulations reported here has been devoted to verification of the transition from an oscillatory to a smooth relaxation profile of the temperature perturbation for different initial wavelengths. Typical results of the simulation are presented in Fig. 1. The FK chains with the same length $N = 1024$, average temperature $T_0 = 1$, and amplitude of the perturbation $A = 0.2$ demonstrate qualitatively different relaxation profiles for different modal wavelengths Z .

Results of the simulations presented in Fig. 2 demonstrate that all three investigated models with the on-site potential clearly exhibit similar transition from diffusive to oscillatory relaxation pattern as the characteristic wavelength decreases. It is possible to distinguish qualitatively three different relaxation patterns: diffusive (curves with $k = 3$), oscillatory (curves with $k = 0, 1$), and crossover (curves with $k = 2$). In other terms, for all these models there exists the critical wavelength scale l^* which separates the oscillatory from the diffusive decay. For the simulations presented here this characteristic scale is

$$l^* \sim 200\text{--}300. \quad (10)$$

Thus, already at this step one can conclude that the hyperbolic behavior can be observed in all three models.

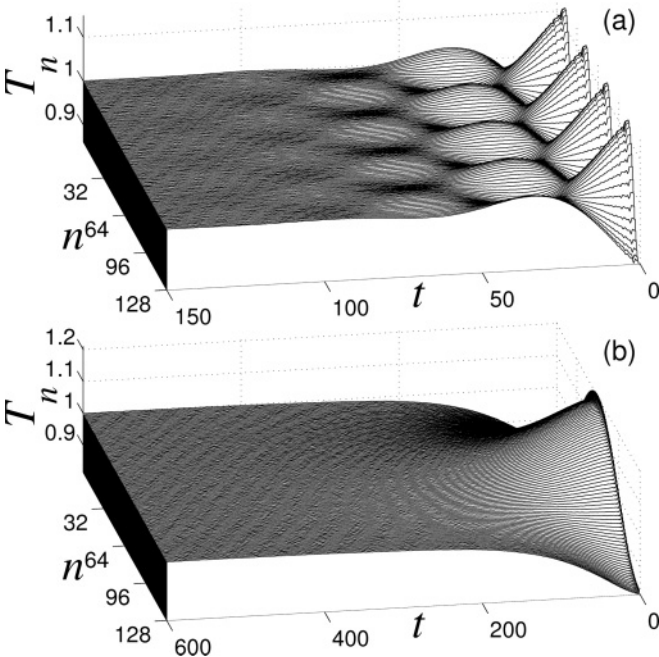


FIG. 1. Relaxation of initial periodic thermal profile in the chain with the FK potential, $N = 1024$, $T_0 = 1$, $A = 0.2$, (a) $Z = 32$, and (b) $Z = 128$. Only part of the chain for n from 1 to 128 is demonstrated.

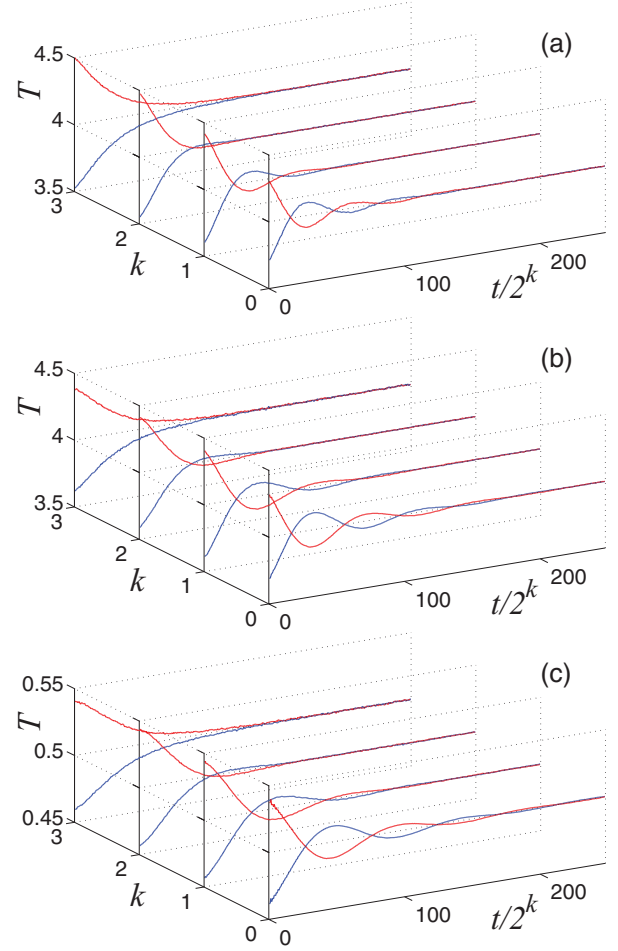


FIG. 2. (Color online) Evolution of the relaxation profile in the chain (length $N = 800$) for $Z = 50, 100, 200$, and 400 ($k = 0, 1, 2$, and 3) with (a) FK potential ($T_0 = 4$, $A = 0.5$); (b) ϕ^4_- potential ($T_0 = 4$, $A = 0.5$); (c) ϕ^4_+ potential ($T = 0.5$, $A = 0.05$). Time dependence of the mode maximum $T(1 + Z/2)$ [red (gray) lines] and minimum $T(1)$ [blue (black) lines] are depicted. Note that the time scales are different for each curve in order to fit them into one figure.

The wide range obtained in Eq. (10) is due to relatively small chain length; this simulation is sufficient to reveal the existence of the transition between the decay patterns, but not sufficient for more or less exact estimation of the critical wavelength scale. In the models with conserved momentum the critical wavelength strongly depends on the average temperature [38]. One can conjecture that similar dependence exists in the models with the on-site potential. To verify this conjecture, we have performed more exact measurements of l^* (for longer chains, up to 10 000 particles, and with higher resolution) for all three models. The results are presented in Fig. 3. As the temperature decreases, the crossover length l^* increases monotonously. This finding is in line with the observation [37] that the second sound waves are observed only for relatively low temperatures of the chain.

IV. LINEARITY OF THERMAL RELAXATION PROFILES

To verify whether the macroscopic equations of the nonstationary heat conduction for given models may be assumed as

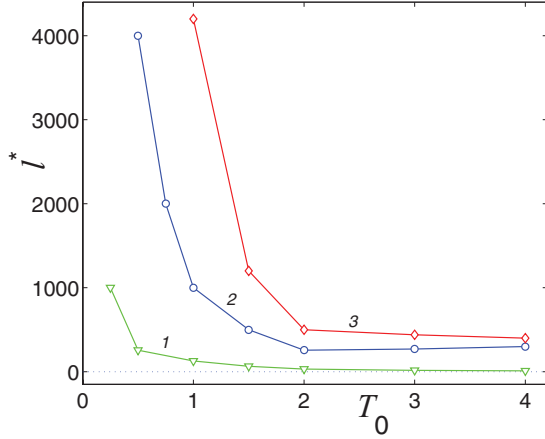


FIG. 3. (Color online) Dependence of the critical wavelength l^* on average temperature T_0 of the chain with ϕ^4+ substrate (curve 1), FK substrate (curve 2), and ϕ^4- substrate potential (curve 3).

linear, we have simulated the evolution of initial temperature distribution (5) with varying amplitude of the perturbation A , keeping all other parameters fixed. Then, the value $\Delta T_n(t) = [T_n(t) - T_0]/A$ is plotted versus time. If the results coincide for different values of A , then it is possible to conclude that the relaxation of the thermal perturbations can be described by a linear equation. In Fig. 4 the simulation results for the FK model are demonstrated.

For all regimes of the relaxation, one barely sees any difference for the relaxation profiles with different initial

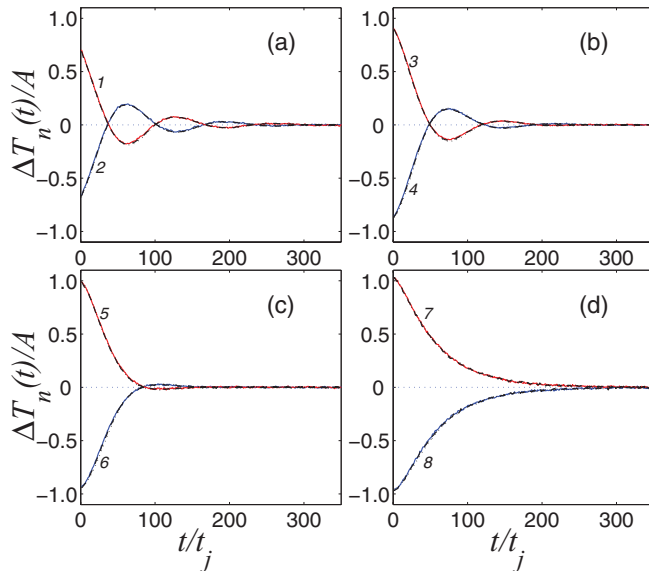


FIG. 4. (Color online) Dependence of rescaled temperature amplitude $\Delta T_n(t)/A = (T_n(t) - T_0)/A$ on rescaled time t/t_j for FK chain: (a) $Z = 50$, $t_j = 0.5$; (b) $Z = 100$, $t_j = 1$; (c) $Z = 200$, $t_j = 2$; (d) $Z = 400$, $t_j = 4$. The length $N = 800$, average temperature $T_0 = 4$. Lines 1,3,5,7 [red (gray)] correspond to the minimum of the temperature in the chain $n = 1$, and Lines 2,4,6,7 [blue (black)]– to the maximum $n = Z/2 + 1$. Solid lines correspond to the perturbation amplitude $A = 0.5$, dashed lines– to $A = 1$, dots – to $A = 2$. The time scales are different for each curve in order to fit them at one figure.

amplitudes; this happens despite the fact that the perturbation is by no means small, i.e., it achieves half the average temperature. Quite similar results were obtained also for ϕ^4- and ϕ^4+ chains. So, one can conclude that the process of thermal relaxation in all these models may be described macroscopically with the help of linear equations with rather good accuracy. A similar conclusion was achieved also for the systems with conserved momentum, but with a somewhat different method [38].

This conclusion is not trivial. The models under consideration are essentially nonlinear and it is not completely clear why linear macroscopic equations should be so suitable for the description of thermal relaxation, especially for relatively large perturbation amplitudes.

V. THERMAL RELAXATION IN OSCILLATORY REGIME

In this section we are going to discuss the relationship of the observed relaxation of the thermal perturbations to the microscopic structure of the investigated models. Complete derivation of the heat transfer equations from first principles has not been achieved yet; still, some insight is possible. First of all, it is easy to see that the nonlinearity of the chain is not necessary to explain the relaxation of the thermal perturbations: dispersion of the linear oscillatory waves is enough to account for this phenomenon. Indeed, in a linear chain, if this dispersion would be absent, the system would obey a simple microscopic wave equation; and due to the periodic boundary conditions, the initial perturbation would recover itself exactly after finite time and no relaxation would be observed. However, due to dispersion, different linear modes will have different and, generally speaking, incommensurate phase velocities. Initial thermal perturbation includes, generically, all of these modes and therefore the initial thermal perturbation will never recover itself and the system will relax to the uniform “temperature” distribution. To distinguish this effect from the relaxation caused by the interactions of the modes in the nonlinear chain, we look at the linear models in more detail.

Let us consider the process of the relaxation of thermal waves in an infinite linear chain with the on-site potential. Such a chain will be described by Eq. (6) with the external potential

$$U_L(u) = \omega^2 u^2 / 2. \quad (11)$$

Appropriate equations of motion will take the form

$$\ddot{u}_n + 2u_n - u_{n-1} - u_{n+1} + \omega^2 u_n = 0. \quad (12)$$

For simplicity, let us adopt that the initial temperature distribution is realized through attribution of initial velocities to each particle, with zero initial displacements. By the virial theorem, such a choice will not affect the long-time asymptotics. Namely, the initial conditions for Eq. (12) are formulated as

$$\begin{aligned} u_n(0) &= 0, \quad \dot{u}_n(0) = \eta_n, \quad \langle \eta_n \rangle = 0, \\ \langle \eta_n \eta_m \rangle &= 2[T_0 + A \cos(2\pi n/Z)] \delta_{nm}, \end{aligned} \quad (13)$$

where η_n is a random value with Gaussian distribution according to Eq. (13). The averaging is performed over the ensemble

of the initial conditions. By standard transformations, it is easy to obtain the following solution of Eq. (12):

$$\begin{aligned} \dot{u}_n(t) &= \sum_{m=-\infty}^{\infty} \eta_m G(n-m, t), \\ G(p, t) &= \frac{1}{\pi} \int_0^{\pi} \cos(t\sqrt{\omega^2 + 4\sin^2\mu} - 2p\mu) d\mu. \end{aligned} \quad (14)$$

The temperature distribution at arbitrary moment of time may be presented as

$$\begin{aligned} T_n(t) &= \langle \dot{u}_n^2 \rangle = T_0 + 2Ag_Z(t) \cos(2\pi n/Z), \\ g_Z(t) &= \sum_{p=-\infty}^{\infty} G^2(p, t) \cos(2\pi p/Z). \end{aligned} \quad (15)$$

The time dependence of a given thermal mode is completely governed by the long-time asymptotics of function $g_Z(t)$. For a given linear model with on-site potential it is difficult to perform the exact integrations and summations in Eqs. (14) and (15) (for the case without the on-site potential these expressions can be reduced to compact exact expressions in terms of Bessel functions). Instead, we are going to derive the required asymptotics by the approximate method, taking into account only generic features of the dispersion relation used in Eq. (14). For this sake, let us consider the general Green's function similar to Eq. (14)

$$G_0(p, t) = \frac{1}{\pi} \int_0^{\pi} \cos[tf(\mu) - 2p\mu] d\mu, \quad (16)$$

where $f(\mu)$ is bounded at interval $(0, \pi)$ and has a single inflection point μ^* with a positive first derivative, which satisfies the conditions

$$f''(\mu^*) = 0, \quad f'(\mu^*) > 0, \quad \mu^* \in [0, \pi]. \quad (17)$$

Then, for t large enough, the integral in Eq. (16) can be evaluated by a stationary phase method. The condition of the stationary phase for specific values of p, t is presented as

$$\Omega(\mu, p, t) = tf(\mu) - 2p\mu, \quad \Omega'(\mu_0) = tf'(\mu_0) - 2p = 0. \quad (18)$$

For simplicity, we will consider only the case where Eq. (18) has a unique solution. In the vicinity of this point, the phase is expanded as

$$\begin{aligned} \Omega &= f(\mu_0)t - 2p\mu_0 + \frac{1}{2}f''(\mu_0)t(\mu - \mu_0)^2 \\ &+ \frac{1}{6}f'''(\mu_0)t(\mu - \mu_0)^3 + \dots \end{aligned} \quad (19)$$

Standard evaluation of integral (16) for the case $t \gg p$ takes into account only the terms up to the term with the second derivative in Eq. (19) and leads to the following estimation:

$$G_0(p, t) \sim t^{-1/2}, \quad t \rightarrow \infty. \quad (20)$$

In the vicinity of the inflection point, which is defined by condition $\mu_0 = \mu^*$, the term with the second derivative in expansion (19) will disappear, and one has to take into account the next term in Eq. (19):

$$\Omega = f(\mu^*)t - 2p\mu^* + \frac{1}{6}f'''(\mu^*)t(\mu - \mu^*)^3 + \dots \quad (21)$$

Evaluation of integral (16) with phase expansion (21) will yield

$$\begin{aligned} G_0(p, t) &= \frac{1}{\pi} \int_0^{\pi} \cos[\Omega(\mu, p, t)] d\mu \\ &\sim t^{-1/3} \cos[f(\mu^*)t - 2p\mu^* + \psi] + O(t^{-2/3}), \end{aligned} \quad (22)$$

where ψ denotes constant phase shift. Expansion (22) is valid for $2p/t \approx f'(\mu^*)$. This contribution corresponds to the linear waves with group velocity close to maximum. Estimation (22) suggests, more exactly, that the expansion is valid for the interval of p defined as

$$|p - p^*| \sim (p^*)^{1/3}, \quad p^* = tf'(\mu^*)/2. \quad (23)$$

Due to a slower decrease rate with respect to time, the terms in expansion (15) in the interval of index defined by

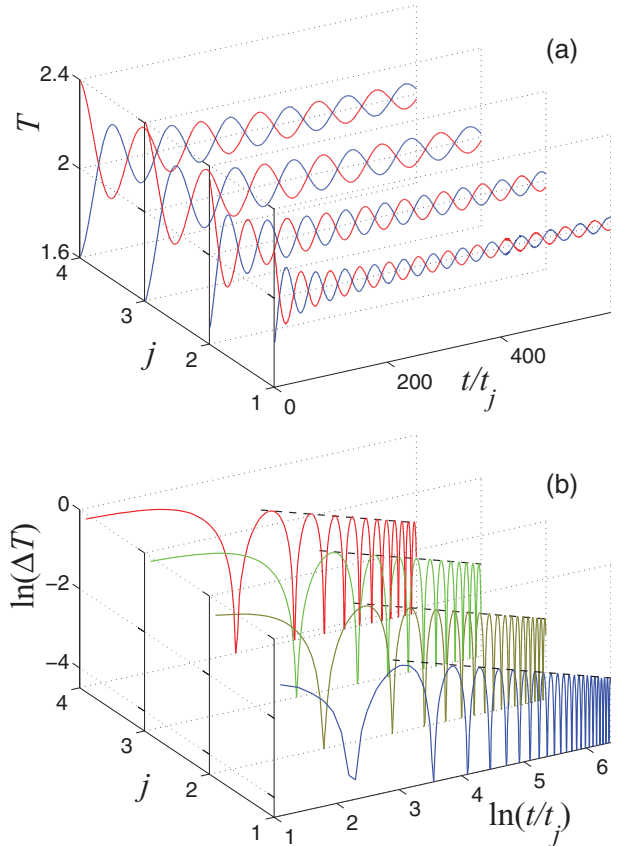


FIG. 5. (Color online) (a) Evolution of the relaxation profile in the linear chain (frequency $\omega = 1$, length $N = 1024$, average temperature $T_0 = 2$, amplitude $A = 0.4$) for $Z = 32, 64, 128$, and 256 ($j = 1, 2, 3$, and 4 ; time scales $t_1 = 1, t_2 = 1.5, t_3 = 2$, and $t_4 = 4$, respectively). Time dependence of the mode minimum T_1 [red (gray) lines] and maximum $T_{Z/2+1}$ [blue (black) lines] are depicted. The time scales are different for each curve in order to fit them into one figure. (b) The same results are presented in double logarithmic coordinates, $\Delta T(t) = |T_1(t) - T_0| + |T_{Z/2+1}(t) - T_0|$. Dashed fitting lines correspond to the power law $\Delta T \sim t^{-0.48}$.

estimation (23) will be the most significant for long-time behavior. Then, the sum in Eq. (15) may be estimated as

$$g_k(t) \sim t^{-2/3} \sum_{p=p^*-(p^*)^{1/3}}^{p^*+(p^*)^{1/3}} \cos\left(\frac{2\pi p}{Z}\right) \times \cos^2[f(\mu^*)t - 2p\mu^* + \psi]. \quad (24)$$

For the most interesting case of relatively small wave numbers, the input of the sum in Eq. (24) will be of order of the square root of the number of participating summands, i.e., of order $(p^*)^{1/6}$. Consequently, with the account of Eq. (23), one finally arrives at the following estimation:

$$g_Z(t) \sim t^{-2/3}(p^*)^{1/6} \sim t^{-1/2}. \quad (25)$$

As it is clear from the treatment, estimation (25) should be rather generic for linear chains. This power-law decay of the thermal mode is illustrated in Fig. 5.

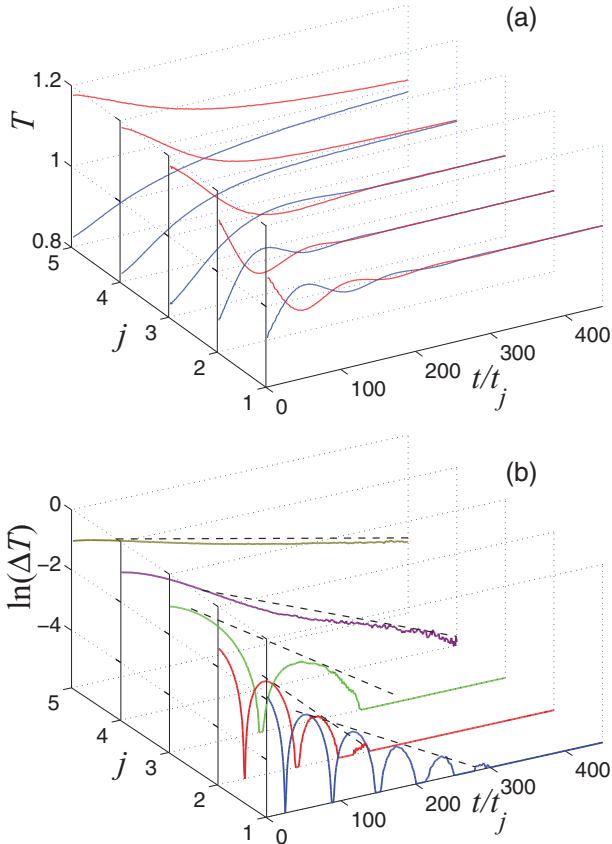


FIG. 6. (Color online) (a) Evolution of the relaxation profile in the ϕ^4+ chain (length $N = 1024$, average temperature $T_0 = 1$, amplitude $A = 0.2$) for $Z = 16, 32, 64, 128$ and 256 ($j = 1, 2, 3, 4$ and 5 ; time scale $t_1 = 0.25, t_2 = t_3 = 0.5, t_4 = 1$, and $t_5 = 2$ respectively). Time dependence of the minimum T_1 [red (gray) lines] and maximum $T_{Z/2+1}$ [blue (black) lines] are depicted. The time scales are different for each curve in order to fit them at one figure. (b) Decay profile of the temperature difference $\Delta T(t) = |T_1(t) - T_0| + |T_{Z/2+1}(t) - T_0|$ in semilogarithmic coordinates. Dashed lines correspond to $\Delta T \sim \exp(-t/t_r)$ with $t_r = 18.9, 22.2, 31.3, 100$ and 370 for $j = 1, 2, 3, 4$ and 5 respectively.

Therefore, we see that the thermal “relaxation” in linear chains obeys a power law rather than an exponential. One can also mention that, quite as expected, the long-time asymptotics is not affected by the difference between the finite chain with periodic boundary conditions used for the simulations and the infinite chain used treated analytically.

This result means that the dispersion of the linear waves brings about slow power-law decay of the thermal perturbation instead of the exponential law expected from known phenomenological macroscopic equations (for instance, both the Fourier law and the CV equation). Thus, the expected exponential relaxation of the thermal perturbations should appear due to nonlinear modal interactions in the chain.

The next point to check is whether the decay of the thermal disturbances in the considered nonlinear models is indeed exponential. For this sake, we simulate the relaxation for different wave numbers k for the ϕ^4+ on-site potential (9). The results are presented in Fig. 6. This simulation clearly demonstrates the exponential character of decay for $\Delta T(t) = |T_1(t) - T_0| + |T_{Z/2+1}(t) - T_0|$:

$$\Delta T(t) \sim \exp(-t/t_r), \quad \text{when } t \rightarrow \infty,$$

However, in Fig. 6 we already can see that the characteristic relaxation time t_r in the oscillatory regime depends on the perturbation wavelength, clearly at odds with the CV law; as it was already mentioned above, the latter suggests that the

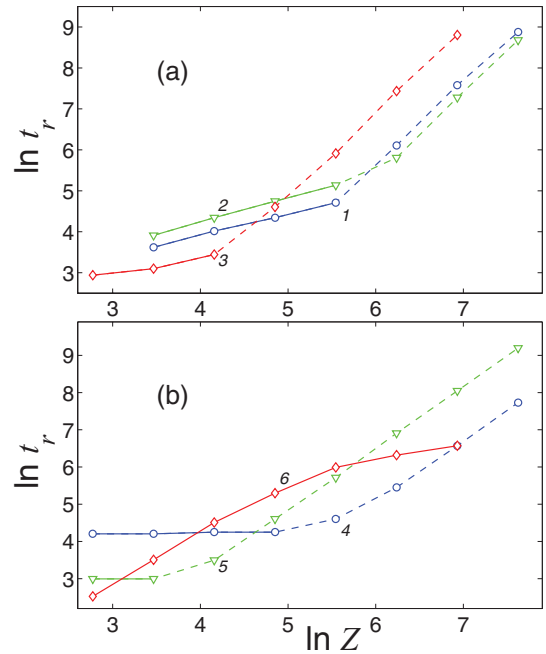


FIG. 7. (Color online) Dependence of the characteristic relaxation time t_r on the period of initial thermal perturbation Z (double logarithmic scale): (a) the models with on-site potential: FK model (line 1, average temperature $T_0 = 2$, perturbation amplitude $A = 0.5$), ϕ^4- model (line 2, $T_0 = 2, A = 0.5$), ϕ^4+ model (line 3, $T_0 = 1, A = 0.2$); (b) the models with conserved momentum [38]: chain of rotators (line 4, $T_0 = 0.5$, line 5, $T_0 = 0.3$) FPU (line 6, $T_0 = 20$). For all models, the solid part of the line corresponds to the oscillatory relaxation pattern and the dashed – to the crossover and monotonous relaxation.

relaxation time in the oscillatory regime should not depend on the wavelength [38]. To further clarify this point, we present in Fig. 7 the dependence of the characteristic relaxation time on the thermal perturbation wavelength for all three models with the on-site potentials studied above, as well as for the models with conserved momentum (FPU and chain of rotators) studied in Ref. [38].

As we can see from these results, two out of three models with the on-site potential (FK and φ^4-) exhibit peculiar scaling of the relaxation time in the oscillatory regime, which conforms to the approximate law

$$\tau_k \sim (N/k)^\beta, \quad (26)$$

with $\beta \approx 0.45$. Similarly, one can suggest that the FPU model obeys similar a scaling law with $\beta \approx 1.4$ for a certain range of the perturbation wavelengths. However, the latter case is more complicated since in the FPU chain it is more difficult to distinguish clearly between the oscillatory and monotonous relaxation patterns [38]. As for the φ^4+ model, the relaxation time also depends on the wavelength of the initial thermal profile, but it is difficult to speak about some peculiar scaling. Only in the chain of rotators does the relaxation time in the oscillatory regime not seem to depend on the wavelength of the temperature perturbation.

VI. CONCLUDING REMARKS

On the basis of the simulations presented above, one can conclude that the one-dimensional models with topologically different substrate potentials exhibit qualitatively similar behavior with respect to nonstationary thermal conductivity. The

thermal relaxation can be quite accurately described by linear equations even for relatively high perturbation amplitudes. All three models demonstrate the transition from oscillatory to diffusive relaxation regimes for growing wavelength of the initial thermal profile. Characteristic crossover wavelength rapidly decreases with the temperature increase.

Quantitative study reveals that no unique relaxation time exists for different spatial harmonics of the initial temperature profile. For some (but not all) of the models, the relaxation times in the oscillatory regime approximately obey scaling law with respect to the wavelength of the initial thermal profile. In particular, it means that neither of the models with the substrate potential obeys the well-known Cattaneo-Vernotte (CV) equation.

All studied models are known to obey the Fourier law in the thermodynamical limit. The fact that the CV law is not suitable for description of the nonstationary heat transfer in these systems is rather surprising. Still, at this stage one cannot claim that the scaling exponents observed here are in any sense universal; a lot of further analysis is required. Scaling relationship (26) suggests that the macroscopic equations describing the nonstationary heat conduction in these models should include fractional derivatives. It is somewhat surprising that such fractional terms should appear as hyperbolic corrections to common Fourier law.

The chain of rotators turns out to be “exceptional”: it seems to obey the CV law both for the long and the short wavelengths of the temperature distribution. This result means that even the models with convergent heat conduction can behave in a different manner when the nonstationary thermal relaxation is considered.

-
- [1] S. Lepri, R. Livi, and A. Politi, *Phys. Rep.* **377**, 1 (2003).
 [2] F. Bonetto, J. L. Lebowitz, and L. Rey-Bellet, in *Mathematical Physics 2000*, edited by A. S. Fokas *et al.* (Imperial College Press, London, 2000), p. 128.
 [3] R. E. Peierls, *Quantum Theory of Solids* (Oxford University, Oxford, 1955).
 [4] E. Fermi, J. Pasta, and S. Ulam, (1955) Studies of Nonlinear Problems. Los Alamos report LA-1940, published later in Collected Papers of Enrico Fermi, edited by E. Segre, Vol. 2 (University of Chicago Press, 1965), pp. 978–988.
 [5] S. Lepri, R. Livi, and A. Politi, *Europhys. Lett.* **43**, 271 (1998).
 [6] B. Hu, B. Li, and H. Zhao, *Phys. Rev. E* **61**, 3828 (2000).
 [7] C. Giardinà, R. Livi, A. Politi, and M. Vassalli, *Phys. Rev. Lett.* **84**, 2144 (2000).
 [8] O. V. Gendelman and A. V. Savin, *Phys. Rev. Lett.* **84**, 2381 (2000).
 [9] A. V. Savin and O. V. Gendelman, *Phys. Rev. E* **67**, 041205 (2003).
 [10] O. V. Gendelman and A. V. Savin, *Phys. Rev. Lett.* **92**, 074301 (2004).
 [11] E. Pereira and R. Falcao, *Phys. Rev. Lett.* **96**, 100601 (2006).
 [12] G. Santhosh and D. Kumar, *Phys. Rev. E* **77**, 011113 (2008).
 [13] A. V. Savin, G. P. Tsironis, and X. Zotos, *Phys. Rev. B* **75**, 214305 (2007).
 [14] B. Hu and L. Yang, *Chaos* **15**, 015119 (2005).
 [15] K. Saito and A. Dhar, *Phys. Rev. Lett.* **104**, 040601 (2010).
 [16] H. Shiba and N. Ito, *J. Phys. Soc. Jpn.* **77**, 054006 (2008).
 [17] D. D. Joseph and L. Preziosi, *Rev. Mod. Phys.* **61**, 41 (1989).
 [18] D. D. Joseph and L. Preziosi, *Rev. Mod. Phys.* **62**, 375 (1990).
 [19] D. S. Chandrasekhararaiiah, *Appl. Mech. Rev.* **39**, 355 (1986).
 [20] D. S. Chandrasekhararaiiah, *Appl. Mech. Rev.* **51**, 705 (1998).
 [21] P. Heino, *Journal of Computational and Theoretical Nanoscience* **4**, 896 (2007).
 [22] D. Jou, J. Casas-Vazquez, and G. Lebon, *Extended Irreversible Thermodynamics*, 4th ed. (Springer, New York, 2010).
 [23] C. Cattaneo, *Comptes rendus de l’Académie des sciences* **247**, 431 (1958).
 [24] P. Vernotte, *Comptes rendus de l’Académie des sciences* **246**, 3154 (1958).
 [25] P. Antaki, *Machine Design* **67**, 116 (1995).
 [26] C. I. Christov and P. M. Jordan, *Phys. Rev. Lett.* **94**, 154301 (2005).
 [27] J. Shiomi and S. Maruyama, *Phys. Rev. B* **73**, 205420 (2006).
 [28] S. T. Huxtable, D. G. Cahill, S. Shenogin, L. Xue, R. Ozisik, P. Barone, M. Usrey, M. S. Strano, G. Siddons, M. Shim, and P. Keblinski, *Nat. Mater.* **2**, 731 (2003).
 [29] D. H. Tsai and R. A. MacDonald, *Phys. Rev. B* **14**, 4714 (1976).

- [30] S. Volz, J. B. Saulnier, M. Lallemand, B. Perrin, P. Depondt, and M. Mareschal, *Phys. Rev. B* **54**, 340 (1996).
- [31] D. W. Tang and N. Araki, *International Journal of Thermophysics* **18**, 493 (1997).
- [32] B. Y. Cao and Z. Y. Guo, *J. Appl. Phys.* **102**, 053503 (2007).
- [33] S. G. Volz, *Phys. Rev. Lett.* **87**, 074301 (2001).
- [34] B. C. Daly, H. J. Maris, K. Imamura, and S. Tamura, *Phys. Rev. B* **66**, 024301 (2002).
- [35] S. Flach and G. Mutschke, *Phys. Rev. E* **49**, 5018 (1994).
- [36] T. Schneider and E. Stoll, *Phys. Rev. B* **18**, 6468 (1978).
- [37] F. Piazza and S. Lepri, *Phys. Rev. B* **79**, 094306 (2009).
- [38] O. V. Gendelman and A. V. Savin, *Phys. Rev. E* **81**, 020103(R) (2010).